Experimental Estimation of the Local Convective Heat Transfer in a Corrugated Tube under the Laminar Flow Regime

Surafel Kifle Teklemariam[1*], Fabio Bozzoli[2], Luca Cattani[1,3]

[1] Department of Engineering for Industrial Systems and Technologies, University of Parma, I-43124 Parma, Italy
[2] Department of Industrial Engineering, University of Florence, 50139 Florence, Italy
[3] SITEIA.PARMA Interdepartmental Centre, University of Parma, I-43124 Parma, Italy

* Correspondence: Surafel Kifle Teklemariam (Surafel.teklemariam@unipr.it)

Citation: S. K. Teklemariam, F. Bozzoli, and L. Cattani, "Experimental estimation of the local convective heat transfer in a corrugated tube under the laminar flow regime," *Int. J. Comput. Methods Exp. Meas.*, vol. 13, no. 4, pp. 749–757, 2025. https://doi.org/10.56578/ijcmem130401.

Abstract: Convection heat transfer enhancement techniques play a vital role in many industrial thermal processing applications, including food thermal processing, and the pharmaceutical, and chemical manufacturing industries. These techniques contribute to reducing the size and cost of heat exchangers, conserving energy, improving product quality, and enhancing both energy efficiency and thermal performance. Among passive solutions, corrugated wall tubes are widely adopted in heat exchangers for such applications. This study applies the inverse heat conduction problem (IHCP) method combined with infrared thermography data to estimate the local temperature and convective heat transfer coefficient distributions for forced convection in a transversally corrugated wall tube with high viscosity fluid flow under laminar conditions. The IHCP is solved within the corrugated wall domain using measured external wall temperatures as input. Thermal performance was evaluated over a Reynolds number range of 290–1200. The findings showed that at Re < 350, irregular local temperature and convective heat transfer distributions led to reduced thermal efficiency, unreliable sterilization, and increased microbial risk, whereas for 650 < Re < 1200, thermal efficiency improved significantly. These findings support the development of more efficient heat exchanger designs, offering significant benefits to industries requiring precise thermal management.

Keywords: Corrugation profiles; Heat-transfer enhancement; Inverse heat conduction problem; Infrared thermography; Thermal processing

1 Introduction

Thermal processing represents a critical step across various industrial sectors, including food and pharmaceuticals. In the food and beverage industries, thermal pasteurization is commonly applied to inactivate spoilage microorganisms and stabilize the product for an extended shelf life. In the pharmaceutical industry, thermal processing is an integral part of manufacturing practices, ensuring product safety, efficacy, and process efficiency through multiple applications, such as sterilization, dehydrogenation, and controlled heat treatment during production.

The integration of advanced heat exchanger technologies, modeling efforts, and innovative heating techniques has led to significant enhancements in product quality and process reliability in these industries. However, thermal treatment of high-viscosity fluids presents several unique challenges that require careful design and analysis to ensure uniform and efficient heat transfer. Due to their high viscosity, internal flows are often dominated by conduction rather than convection, leading to non-uniform temperature distributions during processing. Understanding the relationship between fluid viscosity, flow regime, and heat transfer is vital for designing more efficient thermal devices.

Heat transfer can be enhanced using three main techniques categories: active methods, which rely on mechanical aids or electrostatic fields; passive techniques, which do not require external power; and compound techniques, which combine two or more different methods. At present, all three techniques have recently gained importance in heat exchangers and various other applications to achieve compact, efficient, and cost-effective thermal transport devices [1]. Since these techniques do not rely on external power, they are ideal for industrial applications. In

addition, when updating or modifying an existing heat exchanger, passive methods provide quicker and simpler solutions than active techniques [2].

Corrugation is a method used within passive heat transfer enhancement techniques [1, 2]. It is significant and widely adopted in various applications, such as nuclear reactor cooling, refrigeration, heat exchangers, and other industrial systems [1], by incorporating the benefits of extended surfaces, flow turbulators, and artificial roughness [2]. Heat exchangers with corrugated tubes are commonly used for processes such as pasteurization, sterilization, and other thermal treatments [3].

Investigating the behavior of corrugated tubes under laminar flow conditions is essential for enhancing the efficiency of heat exchangers, especially in systems where low Reynolds numbers keep the flow predominantly laminar. These corrugated structures promote fluid mixing and interrupt the thermal boundary layer, which enhances convective heat transfer with a limited increase of pressure losses.

In this study, an experimental investigation of the thermal performance of a transversely corrugated wall tube was carried out. The estimation of the local convective heat transfer coefficient at the fluid–inner wall interface was performed by solving the Inverse Heat Conduction Problem (IHCP) within the tube wall domain, using the outer wall temperature distribution as the input parameter. Infrared thermography was employed to capture the local temperature distribution on the external surface of the corrugated wall. The primary aim of this research was to estimate local temperature and convective heat transfer coefficient distributions in a transversely corrugated wall tube under laminar flow, with a focus on high-viscosity fluids relevant to thermal food processing, pharmaceutical, and chemical manufacturing applications. This is particularly relevant in thermal processing and manufacturing operations such as sterilization, and pasteurization, where non-uniform temperature distributions can compromise process effectiveness. For this reason, the local estimation of the convective heat transfer coefficient is especially important for identifying the optimal geometry that maximizes heat transfer performance.

The IHCP poses a significant challenge in thermal analysis and material science due to its inherently ill-posed nature, which involves determining unknown thermal parameters or boundary conditions from measured temperature data over time [4]. The complex relationship between heat transfer and observed thermal responses makes the IHCP particularly important in applications such as induction heating and energy systems, where precise thermal characterization is essential.

Numerous researchers have conducted experimental, numerical, and analytical studies on various corrugated-wall tube configurations in the laminar flow regime, including transversal corrugated tubes [5], helically corrugated-wall tubes [6, 7], and coiled corrugated tubes [8], corrugated tubes, dimpled tubes and wire coils [9], corrugated tubes fitted with twisted tapes [10], and elliptical-axis tubes [11, 12],and Fluted tube [13], to enhance forced convective heat transfer using high-viscosity fluids.

Barba et al. [14] experimentally studied the performance of a helical corrugated-wall tube in the laminar flow regime using ethylene glycol as the working fluid. They found that, for Reynolds numbers ranging from 100 to 800, the heat transfer enhancement and the increase in friction factor were in the ranges of 4.27–16.79% and 1.83–2.45%, respectively.

Al-Haidari and Al-Obaidi [15] studied the numerical modeling of corrugated-wall tubes and concluded, based on computational fluid dynamics (CFD) results, that corrugated tubes with two-phase fluid flow achieved better thermal performance than smooth tubes.

Rozzi et al. [16] confirmed that helically corrugated tubes effectively enhance convective heat transfer for Reynolds numbers ranging from about 800 to the transitional flow regime, using whole milk, cloudy orange juice, apricot puree, and apple puree as working fluids under both heating and cooling conditions.

Saha [17] investigated the thermal performance of a helical corrugated-wall tube combined with a helical screw tape, using oil as the working fluid. They observed that the combination of helical corrugations and helical screw tape enhanced the thermal performance compared to when each was used individually, for Reynolds numbers between 20 and 900, while the friction factor increased by 10 to 50%.

Bozzoli et al. [18] experimentally investigated cross-helix corrugated-wall tubes to enhance forced convective heat transfer in food processing applications. They found that increasing the corrugation depth significantly improved thermal performance, with the optimal configuration achieving up to three times higher heat transfer than conventional single-helix tubes, particularly for Reynolds numbers between 200 and 2000.

2 Experimental Methodology and Setup

2.1 Geometry Profile and Experimental Setup

In this paper, a transversally corrugated stainless-steel pipe (AISI 304) was tested. The pipe's dimensions are as follows: length: 3 meters, thickness: 1 mm, outer diameter: 16 mm, with a corrugation profile featuring a 16 mm pitch and 1 mm depth. A detailed image of the corrugation profile is shown in Figure 1.

The full length of the pipe is divided into three sections: inlet, heating, and outlet, with ethylene glycol as the working fluid. The 1 m inlet section allows the working fluid to achieve fully developed flow. In the 1.84 m heating

section, two steel fin electrodes are welded and powered by an HP 6671A supply, operating over 0–220 V and 0–8 A.

Figure 1. The tested transversal wall corrugated pipe

The working fluid was continuously circulated by a volumetric pump into a holding tank, from which it entered the corrugated tubes. After passing through the tubes, the fluid returned to the storage tank to repeat the cycle. A secondary heat exchanger, supplied with city water, was used to maintain a constant inlet temperature of the working fluid. This setup facilitated the investigation of the heat transfer performance of the tube under the condition of uniform internal heat generation by the Joule effect in the wall.

To minimize heat exchange with the atmosphere, the investigated tube was fully insulated using a double layer of expanded polyurethane. For local heat transfer estimation, a portion of approximately 16 cm of thermal insulation was removed from the heated section of the tube's external wall, exposing the surface to the infrared thermography camera. This portion was coated with a thin film of opaque acrylic paint with a known effective emissivity value of 0.95. The effective emissivity of the paint was estimated at different known temperatures.

The surface temperature distribution was measured using an infrared thermography camera (FLIR SC7000) with a 640 × 512-pixel sensor, a sensitivity of 20 mK at 303 K, and an accuracy of ± 1 K, as specified by the manufacturer. By rotating the infrared camera around the axis of the painted portion, six images were collected to obtain a temperature map of the entire external wall of the tube from angles of ± 30°.

Once the system reached thermal steady-state conditions, thermal images were captured at three different Reynolds numbers: Re = 300, 700, and 1100. The acquisition time for each image was set to 0.4s with a frame rate of 25 Hz, resulting in each image representing the average of 10 frames to minimize acquisition noise.
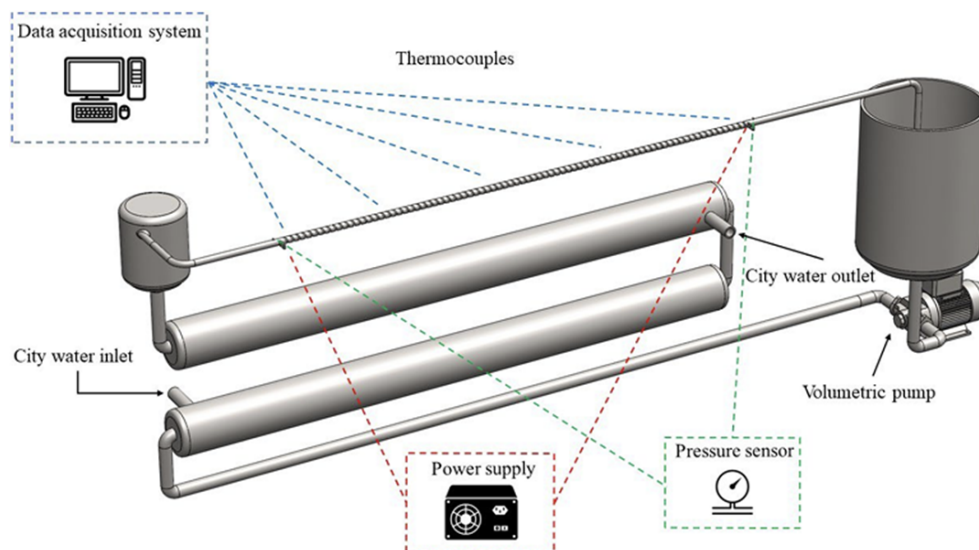

Figure 2. Layout of the experimental setup

The images were cropped, processed using perspective correction algorithms, and combined with MATLAB to generate a continuous temperature distribution along the tube wall as a function of the circumferential angular coordinate. Image processing was complicated by the non-flat nature of the observed surface. To address this, the method described in reference [19], was employed to correct optical distortions in the captured images caused by surface curvature. A visual layout of the experimental setup, as shown in Figure 2, is presented.

T-type thermocouples were employed to measure the temperature of the fluid at the inlet and outlet sections. These thermocouples were carefully calibrated and connected to a multichannel ice point reference, specifically the KAYE K170–50℃, to ensure accurate and precise temperature measurements throughout the experiment.

The bulk temperature at any location along the heat transfer section was estimated from the power supplied to the tube, assuming a uniform distribution along the heat transfer surface. The volumetric flow rate was determined

by measuring the mass of fluid exiting the test section over a known time interval, with data acquisition carried out using a high-precision multimeter interfaced with a personal computer. A support frame, designed to maintain the optical axis of the infrared thermographic camera perpendicular to the tube axis during all image captures, was used to minimize perspective artifacts during acquisition (see Figure 3).
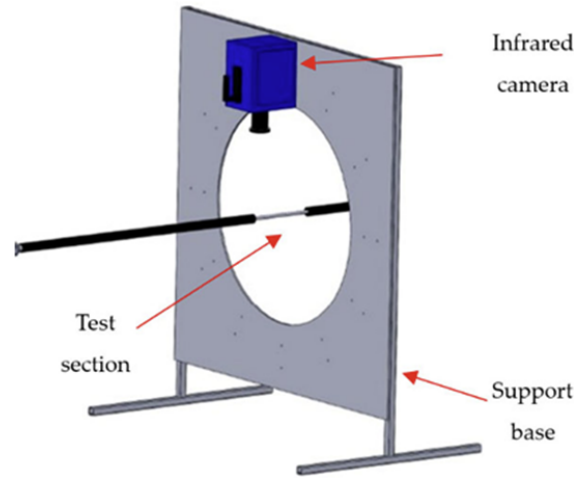

Figure 3. Infrared thermography setup

2.2 Estimation Procedure

In the present study, the forced convective heat transfer performance of a transversally corrugated tube was assessed in terms of the local convective heat transfer coefficient and the Nusselt number. The experimental investigation was conducted by varying the Reynolds number in the range 300–1100:

$$R_e = \frac{4\dot{m}}{\pi \mu D_{int}} \tag{1}$$

where, $\dot{m}$ represents the mass flow rate, and D_{emv} and μ are the internal diameter of the pipe and the dynamic viscosity of the fluid at the average temperature, respectively.
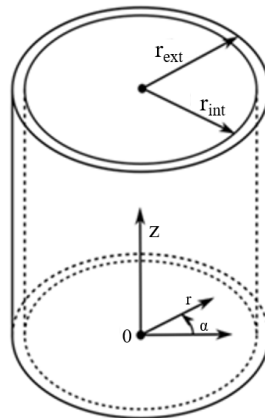

Figure 4. Coordinates system

The physical model involves steady-state heat conduction in the wall of a cylindrical tube (as shown in Figure 4). Based on the temperature distribution obtained across the entire tube surface, as captured by the thermographic infrared camera, the local convective heat transfer coefficient was determined by solving the inverse heat conduction problem (IHCP) within the wall domain. In this domain, the energy balance is governed by the steady-state heat conduction equation, expressed as:

$$k\nabla^2 T + q_g = 0 \tag{2}$$

where, q_g is the heat generated per unit volume in the tube wall, which has a thermal conductivity k. The energy balance equation is governed by the following two boundary conditions:

$$-k\frac{\partial T}{\partial r} = \frac{(T - T_{env})}{R_{env}}, r = r_{ext} \tag{3}$$

$$-k\frac{\partial T}{\partial r} = h_{int}(T - T_b), r = r_{int} \tag{4}$$

where, T_{env} is the ambient temperature, R_{env} is the total hea transfer resistance between the environment, and the tub wall and T_b is the local bulk fluid temperature. By applyin the thin-wall approximation, it was assumed that th temperature on the outer surface was identical to that on th inner surface.

$$(\alpha, r, z) \cong T(\alpha, r_{int}, z) \cong T(\alpha, r_{ext}, z) \tag{5}$$

The thin-wall approximation is valid when the Biot number is less than 0.1 [20]. This condition was confirmed for all the tests performed.
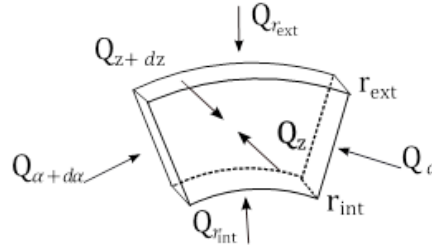

Figure 5. A portion of the test section

Based on the infinitesimal cylindrical element shown in Figure 5, the governing local energy balance equation with an internal source term q_g for the tube section in steady state is given by:

$$Q_{\alpha+d\alpha} + Q_\alpha + Q_{r_{int}} + Q_{r_{ext}} + Q_{z+dz} + Q_z + q_g = 0 \tag{6}$$

After expressing all the terms in Eq. (6) and applying the simplifications detailed in [19], the local convective heat transfer coefficient at the wall–working fluid interface is given by:

$$h_{int} = \frac{k \cdot \ln\left(\frac{r_{ext}}{r_{int}}\right)\frac{\partial^2 T}{\partial \alpha^2} + \frac{k}{2}\left(r_{ext}^2 - r_{int}^2\right)\frac{\partial^2 T}{\partial z^2} - \frac{r_{ext}}{R_{env}}(T - T_{env}) + \frac{a_g}{2}\left(r_{ext}^2 - r_{int}^2\right)}{r_{int} \cdot (T - T_b)} \tag{7}$$

In the presence of discrete noisy experimental data, Eq. (7) produces inaccurate results [21], because the second-order derivative operator is highly sensitive to minor variations in the input data, which are amplified by the destructive nature of noise [4]. An effective solution to these issues is to filter out the noise from the raw temperature data, facilitating the direct calculation of its Laplacian. Bozzoli et al. [21] have investigated the effectiveness of the Gaussian kernel in this approach. The transfer function in the 2-D frequency domain of this type of filter can be expressed as follows:

$$H(u,v) = e^{-\left(u^2+v^2\right)/2u_c^2} \tag{8}$$

where, u_c is the cutoff frequency, assumed to be equal along the u and v coordinates. In practical applications, the optimal cutoff frequency for each filter is not pre-determined: in the present paper it is chosen using the criterion provided by the discrepancy principle, originally formulated by Morozov [22].

3 Results and Discussion

In this research, the performance of a transversally corrugated tube is experimentally analyzed under laminar flow conditions. The evaluation is carried out by studying forced convective heat transfer within a Reynolds number range of 300–1100, using ethylene glycol as the working fluid. To aid understanding, Figure 6 presents a schematic based on infrared (IR) thermography, showing the corrugation position and fluid flow direction (fluid flowing from left to right). The angular coordinate ($\alpha = \pi$ in the circumferential direction is defined as $0 < \alpha < \pi$ and $-\pi < \alpha < 0$ for the top and bottom wall surfaces of the investigated tube, respectively.

Using the measured temperature distribution and applying the IHCP approach described in the previous section, the local convective heat transfer coefficient at the outer wall surface can be determined. In Figure 7, the filtered temperature maps across the axial length (z) and the circumference (α) are presented. These maps were obtained by applying the Gaussian filter (Eq. (8)) to the raw temperature distributions for selected cases of Re $\approx$ 300, 700, and 1100 on the transversal corrugated tube. As the Reynolds number rises, the fluid maintains laminar flow through the corrugated, however its momentum also increases.
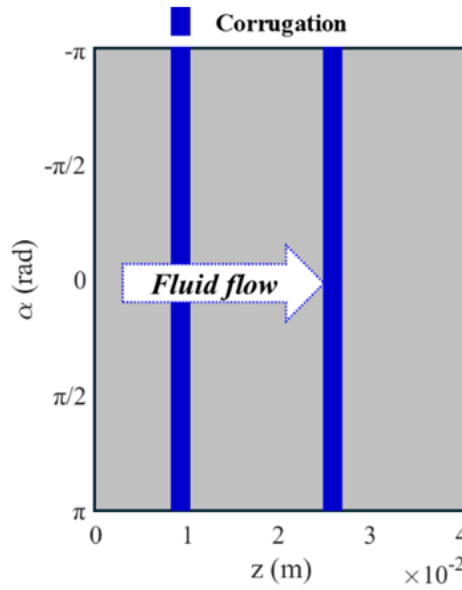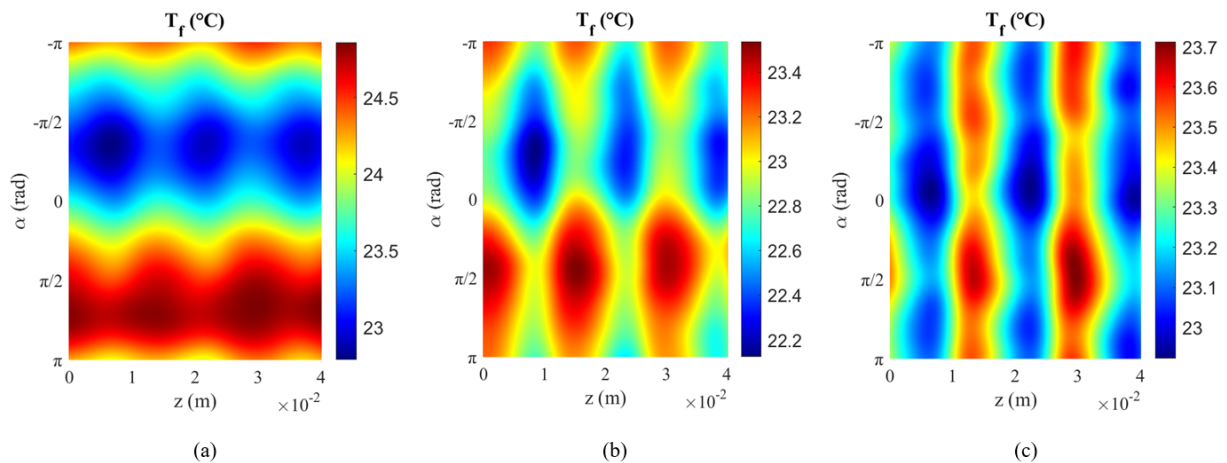

Figure 6. Corrugation position and flow direction

Figure 7. Filtered temperature distributions at the following Reynolds numbers: (a) Re = 300; (b) Re = 700; and (c) Re = 1100

At Re = 300, the flow behavior becomes difficult to characterize. In this Reynolds number range, weak secondary flows develop, leading to uneven fluid mixing and a non-uniform temperature distribution along the circumferential direction of the corrugated tube. Higher temperature variations were observed on the upper half of the tube wall (top surface, $0 < \alpha < \pi$) compared to the lower half (bottom surface, $-\pi < \alpha < 0$), as shown in Figure 7a. However, at Re

= 700, the flow appears to be in the transitional regime (see Figure 7b), exhibiting stronger secondary flows compared to Re = 300. At Re = 1100, a local maximum in the wall temperature distribution is clearly visible immediately after the corrugation. A more uniform temperature distribution is shown, and enhanced efficiency is achieved. It is driven by stronger secondary flows that optimize overall thermal performance, as compared to the lower Reynolds number values (see Figure 7c).

In Figure 8, the local spatial variations of the convective heat transfer are presented for the investigated transversally corrugated tube. The results show a local maximum near the crest and a local minimum downstream of the corrugation. This behavior can be attributed to the disturbance of the boundary layer caused by the fluid encountering roughness along its path, as well as the formation of a recirculation zone that develops downstream of the corrugated surface. The distribution of the local convective heat transfer coefficient is non-uniform, showing a larger difference between the minimum and maximum values at lower Reynolds numbers (see Figure 8a and Figure 8b). In contrast, at Re = 1100, the local heat transfer coefficient exhibits a more uniform distribution, with a reduced difference between the highest and lowest values, promoting a higher heat transfer enhancement compared to lower Reynolds number values (see Figure 8c).
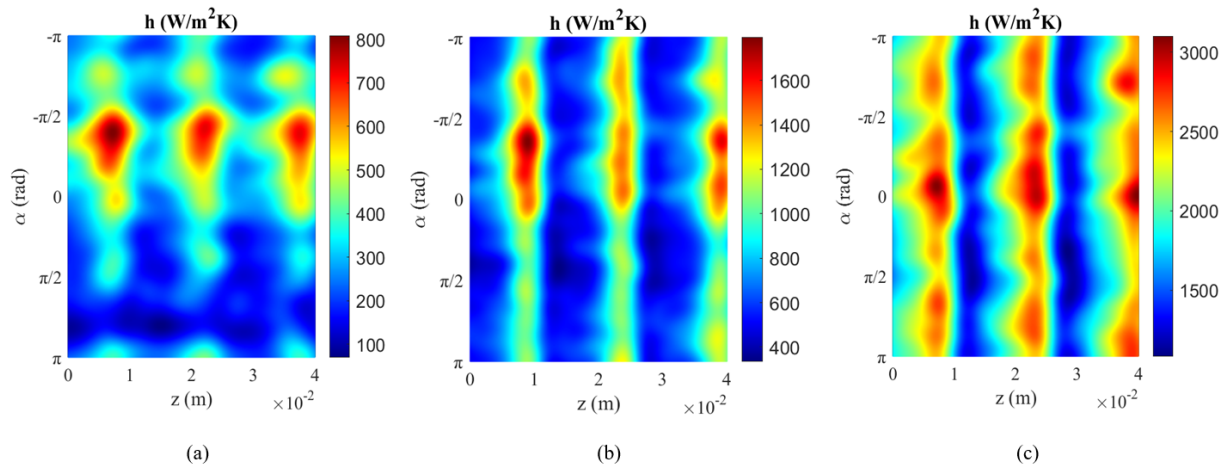

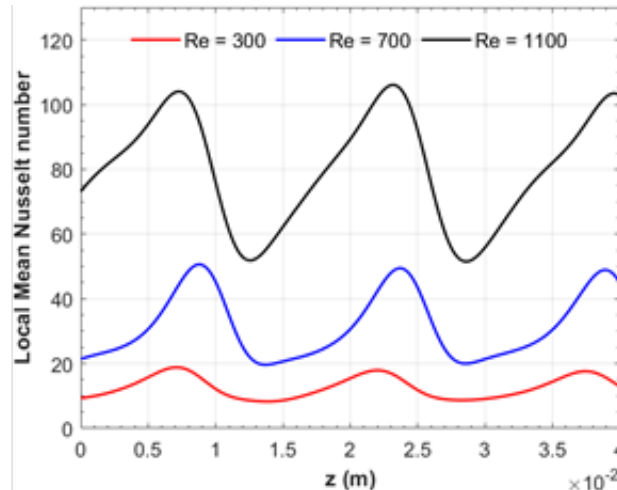**Figure 8.** Local convective heat transfer distributions: (a) Re = 300; (b) Re = 700; and (c) Re = 1100

Figure 9. The local Mean Nusselt distributions at Re = 300, Re = 700, Re = 1100

The local mean Nusselt number distribution at different Reynolds numbers is presented for the Transversally corrugated tube. For all the Reynolds numbers investigated, the local average Nusselt number reached its maximum value in the regions between the corrugations and decreased immediately after the corrugation crest. As the Reynolds number increases, the local average Nusselt number rises due to higher flow velocity and enhanced convective effects within the laminar regime (see Figure 9).

4 Conclusions

In this research, the local thermal performance of a transversally corrugated tube has been experimentally investigated. The estimation technique was experimentally investigated under a fully developed laminar flow regime across a range of Reynolds numbers (300–1100), using ethylene glycol as the working fluid. The results show non-uniform temperature and local convective heat transfer coefficient distributions at lower Reynolds numbers (Re = 300 and 700), due to the minimal mixing in the flow. In contrast, at higher Reynolds numbers (Re = 1100), a more uniform distribution is observed. It is really interesting for applications where local temperature uniformity in the heating process is essential, particularly in the food industry, where such passive heat transfer enhancement solutions are widely used.

Data Availability

The data used to support the findings of this study are available from the corresponding author upon request.

Conflicts of Interest

The authors declare that they have no conflicts of interest.

References

[1] Z. S. Kareem, M. M. Jaafar, T. M. Lazim, S. Abdullah, and A. F. Abdulwahid, "Passive heat transfer enhancement review in corrugation," *Exp. Therm. Fluid Sci.*, vol. 68, pp. 22–38, 2015. https://doi.org/10.1016/j.expthermflusci.2015.04.012

[2] K. Navickaitė, L. Cattani, C. R. Bahl, and K. Engelbrecht, "Elliptical double corrugated tubes for enhanced heat transfer," *Int. J. Heat Mass Transf.*, vol. 128, pp. 363–377, 2019. https://doi.org/10.1016/j.ijheatmasstransfer.2018.09.003

[3] F. Bozzoli, L. Cattani, S. Rainieri, F. S. Bazán, and L. S. Borges, "Estimation of the local heat transfer coefficient in coiled tubes: Comparison between Tikhonovregularization method and Gaussian filtering technique," *Int. J. Numer. Methods Heat Fluid Flow*, vol. 27, no. 3, pp. 575–586, 2017. https://doi.org/10.1108/hff-03-2016-0097

[4] J. V. Beck, B. Blackwell, and C. R. S. Clair, *Inverse Heat Conduction: Ill-Posed Problems.* James Beck, 1985.

[5] C. Chen, Y. T. Wu, S. T. Wang, and C. F. Ma, "Experimental investigation on enhanced heat transfer in transversally corrugated tube with molten salt," *Exp. Therm. Fluid Sci.*, vol. 47, pp. 108–116, 2013. https://doi.org/10.1016/j.expthermflusci.2013.01.006

[6] S. Rainieri, F. Bozzoli, L. Cattani, and G. Pagliarini, "Experimental investigation on the convective heat transfer enhancement for highly viscous fluids in helical coiled corrugated tubes," *J. Phys. Conf. Ser.*, vol. 395, no. 1, p. 012032, 2012. https://doi.org/10.1088/1742-6596/395/1/012032

[7] A. A. R. Darzi, M. Farhadi, and K. Sedighi, "Experimental investigation of convective heat transfer and friction factor of Al_2O_3/water nanofluid in helically corrugated tube," *Exp. Therm. Fluid Sci.*, vol. 57, pp. 188–199, 2014. https://doi.org/10.1016/j.expthermflusci.2014.04.024

[8] S. Rainieri, F. Bozzoli, L. Cattani, and G. Pagliarini, "Compound convective heat transfer enhancement in helically coiled wall corrugated tubes," *Int. J. Heat Mass Transf.*, vol. 59, pp. 353–362, 2013. https://doi.org/10.1016/j.ijheatmasstransfer.2012.12.037

[9] A. García, J. P. Solano, P. G. Vicente, and A. Viedma, "The influence of artificial roughness shape on heat transfer enhancement: Corrugated tubes, dimpled tubes and wire coils," *Appl. Therm. Eng.*, vol. 35, pp. 196–201, 2012. https://doi.org/10.1016/j.applthermaleng.2011.10.030

[10] V. Zimparov, "Prediction of friction factors and heat transfer coefficients for turbulent flow in corrugated tubes combined with twisted tape inserts. Part 1: Friction factors," *Int. J. Heat Mass Transf.*, vol. 47, no. 3, pp. 589–599, 2004. https://doi.org/10.1016/j.ijheatmasstransfer.2003.08.003

[11] B. Li, B. Feng, Y. L. He, and W. Q. Tao, "Experimental study on friction factor and numerical simulation on flow and heat transfer in an alternating elliptical axis tube," *Appl. Therm. Eng.*, vol. 26, no. 17–18, pp. 2336–2344, 2006. https://doi.org/10.1016/J.APPLTHERMALENG.2006.03.001

[12] J. A. Meng, X. G. Liang, Z. J. Chen, and Z. X. Li, "Experimental study on convective heat transfer in alternating elliptical axis tubes," *Exp. Therm. Fluid Sci.*, vol. 29, no. 4, pp. 457–465, 2005. https://doi.org/10.1016/J.EXPTHERMFLUSCI.2004.04.006

[13] Y. T. Kang, R. Stout, and R. N. Christensen, "The effects of inclination angle on flooding in a helically fluted tube with a twisted insert," *Int. J. Multiph. Flow*, vol. 23, no. 6, pp. 1111–1129, 1997. https://doi.org/10.1016/s0301-9322(97)00031-1

[14] A. Barba, S. Rainieri, and M. Spiga, "Heat transfer enhancement in a corrugated tube," *Int. Commun. Heat Mass Transf.*, vol. 29, no. 3, pp. 313–322, 2002. https://doi.org/10.1016/S0735-1933(02)00321-4

[15] S. R. Al-Haidari and A. R. Al-Obaidi, "Extensive investigation of hydrothermal flow and heat performance improvement in a 3D tube based on varying concavity dimple and corrugation turbulator configurations," *Heat Transf.*, vol. 54, no. 5, pp. 3134–3162, 2025. https://doi.org/10.1002/htj.23346

[16] S. Rozzi, R. Massini, G. Paciello, G. Pagliarini, S. Rainieri, and A. Trifiro, "Heat treatment of fluid foods in a shell and tube heat exchanger: Comparison between smooth and helically corrugated wall tubes," *J. Food Eng.*, vol. 79, no. 1, pp. 249–254, 2007. https://doi.org/10.1016/J.JFOODENG.2006.01.050

[17] S. K. Saha, "Thermohydraulics of laminar flow through a circular tube having integral helical corrugations and fitted with helical screw-tape insert," *Chem. Eng. Commun.*, vol. 200, no. 3, pp. 418–436, 2013. https://doi.org/10.1080/00986445.2012.712579

[18] F. Bozzoli, L. Cattani, and S. Rainieri, "Cross-helix corrugation: The optimal geometry for effective food thermal processing," *Int. J. Heat Mass Transf.*, vol. 147, p. 118874, 2020. https://doi.org/10.1016/j.ijheatmasstransfer.2019.118874

[19] F. Bozzoli, L. Cattani, and S. Rainieri, "Effect of wall corrugation on local convective heat transfer in coiled tubes," *Int. J. Heat Mass Transf.*, vol. 101, pp. 76–90, 2016. https://doi.org/10.1016/j.ijheatmasstransfer.2016.04.106

[20] T. L. Bergman, *Fundamentals of Heat and Mass Transfer*. John Wiley & Sons, 2011.

[21] F. Bozzoli, L. Cattani, G. Pagliarini, and S. Rainieri, "Infrared image filtering applied to the restoration of the convective heat transfer coefficient distribution in coiled tubes," *Opto-Electron. Rev.*, vol. 23, no. 1, pp. 107–115, 2015. https://doi.org/10.1515/oere-2015-0004

[22] V. A. Morozov, *Methods for Solving Incorrectly Posed Problems*. Springer Science & Business Media, 2012.

Nomenclature

D	Tube internal diameter, m
r	Radius of the cylinder, m
T	Temperature, K
k	Thermal conductivity, W/m·K
Nu	Nusselt number
h	Convective heat transfer coefficient, W/m^2·K
Re	Reynolds number
q_g	Internal heat generation per unit volume, W/m^3
$\dot{m}$	Mass flow rate, kg/s
R_{env}	Overall heat transfer resistance between the external tube wall and the surrounding environment, m^2·K/W

Greek symbols

α	Angular coordinate, rad
μ	Dynamic viscosity, Pa.s

Subscripts

b	Bulk
env	Environment
ext	External
f	Filtered
int	Internal